# Weight-adjusted DG methods for elastic wave propagation in arbitrary heterogeneous media

Jesse Chan

Department of Computational and Applied Math, Rice University

ICOSAHOM 2018
July 12, 2018

# Collaborators and acknowledgements

- Prof. T. Warburton: Virginia Tech, Department of Mathematics
- Dr. Russell Hewett: TOTAL Research and Technology USA
- Prof. Maarten de Hoop: Rice University, Department of Computational Mathematics
- Khemraj Shukla: Oklahoma State University, Dept. of Geophysics.

# High order DG methods for wave propagation

- Unstructured (tetrahedral) meshes for geometric flexibility.
- Low numerical dissipation and dispersion.
- High order approximations: more accurate per unknown.
- Explicit time stepping: high performance on many-core.

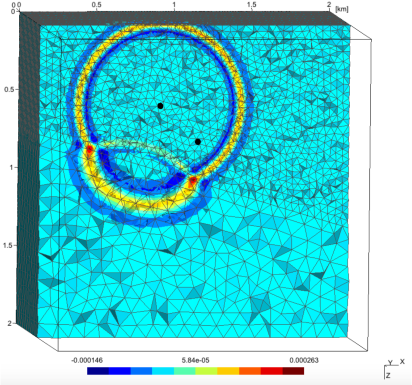


Figure courtesy of Axel Modave.

# High order DG methods for wave propagation

- Unstructured (tetrahedral) meshes for geometric flexibility.
- Low numerical dissipation and dispersion.
- High order approximations: more accurate per unknown.
- Explicit time stepping: high performance on many-core.

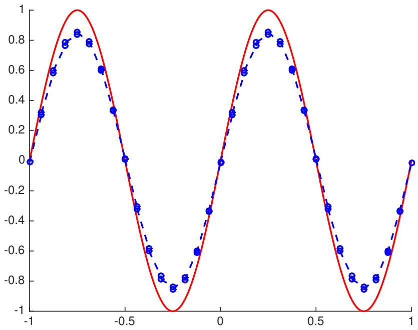


**Fine** linear approximation.

# High order DG methods for wave propagation

- Unstructured (tetrahedral) meshes for geometric flexibility.
- Low numerical dissipation and dispersion.
- High order approximations: more accurate per unknown.
- Explicit time stepping: high performance on many-core.

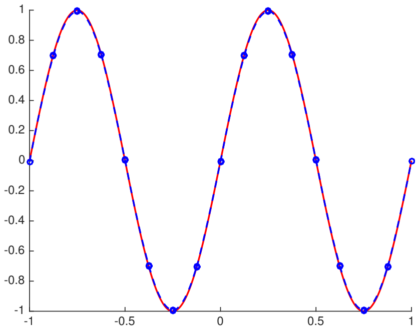


**Coarse** quadratic approximation.

# High order DG methods for wave propagation

- Unstructured (tetrahedral) meshes for geometric flexibility.
- Low numerical dissipation and dispersion.
- High order approximations: more accurate per unknown.
- Explicit time stepping: high performance on many-core.

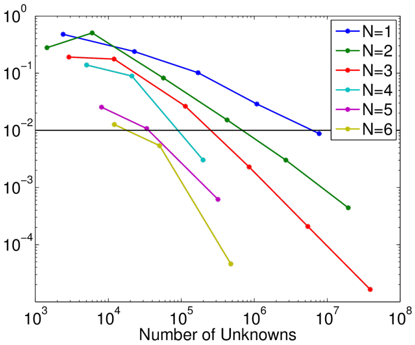


Max errors vs. dofs.

# High order DG methods for wave propagation

- Unstructured (tetrahedral) meshes for geometric flexibility.
- Low numerical dissipation and dispersion.
- High order approximations: more accurate per unknown.
- Explicit time stepping: high performance on many-core.

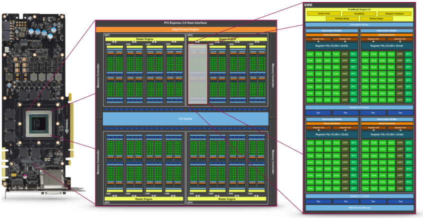

Graphics processing units (GPU).

# Outline

# Outline

# High order methods and arbitrary heterogeneous media

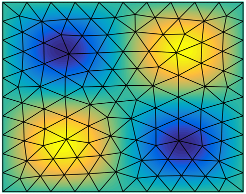

(a) Mesh and exact $c^2$

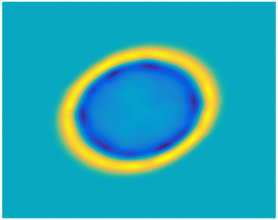

(b) Piecewise const. $c^2$

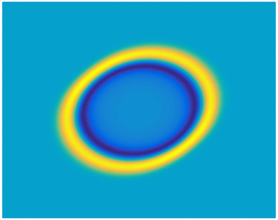

(c) High order $c^2$

- Efficient implementations on **triangular** or **tetrahedral** meshes assume piecewise constant wavespeed $c^2$.
- High order vs constant approx. of media: spurious reflections.
- This talk: generalized mass lumping for DG with provable stability, high order accuracy, simple numerical fluxes (central flux + penalty).

# Energy stable discontinuous Galerkin formulations

- Model problem: acoustic wave equation (pressure-velocity system)

$$\frac{1}{c^2(\boldsymbol{x})}\frac{\partial p}{\partial t} = \nabla \cdot \boldsymbol{u}, \qquad \frac{\partial \boldsymbol{u}}{\partial t} = \nabla p$$

- Local formulation on element $D^k$

$$\begin{aligned}\int_{D^k} \frac{1}{c^2(\boldsymbol{x})}\frac{\partial p}{\partial t} q &= \int_{D^k} \nabla \cdot \boldsymbol{u} q + \frac{1}{2}\int_{\partial D^k} \left( [\![\boldsymbol{u}]\!] \cdot \boldsymbol{n} + \tau_p [\![p]\!] \right) q \\ \int_{D^k} \frac{\partial \boldsymbol{u}}{\partial t} \boldsymbol{v} &= \int_{D^k} \nabla p \cdot \boldsymbol{v} + \frac{1}{2}\int_{\partial D^k} \left( [\![p]\!] + \tau_u [\![\boldsymbol{u}]\!] \cdot \boldsymbol{n} \right) \boldsymbol{v}\end{aligned}$$

- Energy stability (penalty terms weakly enforce continuity conditions)

$$\frac{\partial}{\partial t}\left( \sum_k \int_{D^k} \frac{p^2}{c^2(\boldsymbol{x})} + |\boldsymbol{u}|^2 \right) = -\sum_k \int_{\partial D^k} \tau_p [\![p]\!]^2 + \tau_u [\![\boldsymbol{u} \cdot \boldsymbol{n}]\!]^2 \leq 0.$$

# Semi-discrete formulation and weighted mass matrices

- Weighted mass matrix $\boldsymbol{M}_{1/c^2}$: SPD, induces weighted norm on $\boldsymbol{p}$

$$\left(\boldsymbol{M}_{1/c^2}\right)_{ij} = \int_{D^k} \frac{1}{c^2(\boldsymbol{x})} \phi_j(\boldsymbol{x}) \phi_i(\boldsymbol{x}) \, \mathrm{d}\boldsymbol{x}.$$

- Semi-discrete form: face mass and weak derivative matrices $\boldsymbol{M}_f$, $\boldsymbol{S}_i$.

$$\boldsymbol{M}_{1/c^2} \frac{\mathrm{d}\boldsymbol{p}}{\mathrm{d}t} = \sum_{i=1}^{d} \boldsymbol{S}_i \boldsymbol{u}_i + \sum_{\text{faces}} \boldsymbol{M}^f \boldsymbol{F}_p,$$

$$\boldsymbol{M} \frac{\mathrm{d}\boldsymbol{u}_i}{\mathrm{d}t} = \boldsymbol{S}_i \boldsymbol{p} + \sum_{\text{faces}} \boldsymbol{M}^f \boldsymbol{F}_u.$$

- Must build and factorize $\boldsymbol{M}_{1/c^2}$ separately over each element (unless $c^2$ constant and $\left(\boldsymbol{M}_{1/c^2}\right)^{-1} = c^2 \boldsymbol{M}^{-1}$).

# Weight-adjusted DG: generalized mass lumping

- Weight-adjusted DG (WADG): $\boldsymbol{M}\left(\boldsymbol{M}_{1/w}\right)^{-1}\boldsymbol{M}$ is SPD and an energy stable approximation of weighted mass matrix.

$$\boldsymbol{M}_w \frac{\mathrm{d}\boldsymbol{U}}{\mathrm{d}t} \approx \boldsymbol{M}\left(\boldsymbol{M}_{1/w}\right)^{-1}\boldsymbol{M}\frac{\mathrm{d}\boldsymbol{U}}{\mathrm{d}t} = \text{right hand side}.$$

- Bypasses inverse of weighted matrix $\left(\boldsymbol{M}_w\right)^{-1}$

$$\left(\boldsymbol{M}\left(\boldsymbol{M}_{1/w}\right)^{-1}\boldsymbol{M}\right)^{-1} = \boldsymbol{M}^{-1}\boldsymbol{M}_{1/w}\boldsymbol{M}^{-1}.$$

- Low storage matrix-free application of $\boldsymbol{M}^{-1}\boldsymbol{M}_{1/w}$ using quadrature.

$$\boldsymbol{M} = \boldsymbol{V}_q^T\boldsymbol{W}\boldsymbol{V}_q, \quad \boldsymbol{V}_q = \text{ eval. at quad. pts}, \quad \boldsymbol{W} = \text{ quad. weights}$$
$$\left(\boldsymbol{M}\right)^{-1}\boldsymbol{M}_{1/w}\text{RHS} = \underbrace{\widehat{\boldsymbol{M}}^{-1}\boldsymbol{V}_q^T\boldsymbol{W}}_{\boldsymbol{P}_q}\operatorname{diag}\left(1/w\right)\boldsymbol{V}_q\left(\text{RHS}\right).$$

# WADG and high order accuracy

- Generates norm with same equivalence constants

$$w_{\min} \boldsymbol{u}^T \boldsymbol{M} \boldsymbol{u} \leq \boldsymbol{u}^T \boldsymbol{M}_w \boldsymbol{u} \leq w_{\max} \boldsymbol{u}^T \boldsymbol{M} \boldsymbol{u}$$

- High order accuracy of weighted projection $P_w$, WADG projection $\tilde{P}_w$

$$\left\| u - \tilde{P}_w u \right\|_{L^2} \leq C_w h^{N+1} \|w\|_{W^{N+1,\infty}} \|u\|_{W^{N+1,2}}$$
$$\left\| P_w u - \tilde{P}_w u \right\|_{L^2} \leq C_{w,N} h^{N+2} \|w\|_{W^{N+1,\infty}} \|u\|_{W^{N+1,2}}.$$

- WADG retains high order accuracy for moments: if $v \in P^M$

$$\left| \boldsymbol{v}^T \boldsymbol{M}_w \boldsymbol{u} - \boldsymbol{v}^T \boldsymbol{M}^{-1} \boldsymbol{M}_{1/w} \boldsymbol{M}^{-1} \boldsymbol{u} \right| \leq$$
$$C_w \|w\|_{W^{N+1,\infty}} h^{2N+2-M} \|u\|_{W^{N+1,2}} \|v\|_{L^2}.$$

# WADG and high order accuracy

- Generates norm with same equivalence constants

$$w_{\min}\boldsymbol{u}^T\boldsymbol{M}\boldsymbol{u} \leq \boldsymbol{u}^T\boldsymbol{M}^{-1}\boldsymbol{M}_{1/w}\boldsymbol{M}^{-1}\boldsymbol{u} \leq w_{\max}\boldsymbol{u}^T\boldsymbol{M}\boldsymbol{u}$$

- High order accuracy of weighted projection $P_w$, WADG projection $\tilde{P}_w$

$$\left\|u - \tilde{P}_w u\right\|_{L^2} \leq C_w h^{N+1} \|w\|_{W^{N+1,\infty}} \|u\|_{W^{N+1,2}}$$
$$\left\|P_w u - \tilde{P}_w u\right\|_{L^2} \leq C_{w,N} h^{N+2} \|w\|_{W^{N+1,\infty}} \|u\|_{W^{N+1,2}}.$$

- WADG retains high order accuracy for moments: if $v \in P^M$

$$\left|\boldsymbol{v}^T\boldsymbol{M}_w\boldsymbol{u} - \boldsymbol{v}^T\boldsymbol{M}^{-1}\boldsymbol{M}_{1/w}\boldsymbol{M}^{-1}\boldsymbol{u}\right| \leq C_w \|w\|_{W^{N+1,\infty}} h^{2N+2-M} \|u\|_{W^{N+1,2}} \|v\|_{L^2}.$$

# WADG and high order accuracy

- Generates norm with same equivalence constants

$$w_{\min} \boldsymbol{u}^T \boldsymbol{M} \boldsymbol{u} \leq \boldsymbol{u}^T \boldsymbol{M}^{-1} \boldsymbol{M}_{1/w} \boldsymbol{M}^{-1} \boldsymbol{u} \leq w_{\max} \boldsymbol{u}^T \boldsymbol{M} \boldsymbol{u}$$

- High order accuracy of weighted projection $P_w$, WADG projection $\tilde{P}_w$

$$\left\| u - \tilde{P}_w u \right\|_{L^2} \leq C_w h^{N+1} \left\| w \right\|_{W^{N+1,\infty}} \left\| u \right\|_{W^{N+1,2}}$$
$$\left\| P_w u - \tilde{P}_w u \right\|_{L^2} \leq C_{w,N} h^{N+2} \left\| w \right\|_{W^{N+1,\infty}} \left\| u \right\|_{W^{N+1,2}}.$$

- WADG retains high order accuracy for moments: if $v \in P^M$

$$\left| \boldsymbol{v}^T \boldsymbol{M}_w \boldsymbol{u} - \boldsymbol{v}^T \boldsymbol{M}^{-1} \boldsymbol{M}_{1/w} \boldsymbol{M}^{-1} \boldsymbol{u} \right| \leq$$
$$C_w \left\| w \right\|_{W^{N+1,\infty}} h^{2N+2-M} \left\| u \right\|_{W^{N+1,2}} \left\| v \right\|_{L^2}.$$

# WADG and high order accuracy

- Generates norm with same equivalence constants

$$w_{\min}\boldsymbol{u}^T\boldsymbol{M}\boldsymbol{u} \leq \boldsymbol{u}^T\boldsymbol{M}^{-1}\boldsymbol{M}_{1/w}\boldsymbol{M}^{-1}\boldsymbol{u} \leq w_{\max}\boldsymbol{u}^T\boldsymbol{M}\boldsymbol{u}$$

- High order accuracy of weighted projection $P_w$, WADG projection $\tilde{P}_w$

$$\begin{aligned}\left\|u - \tilde{P}_w u\right\|_{L^2} &\leq C_w h^{N+1} \|w\|_{W^{N+1,\infty}} \|u\|_{W^{N+1,2}} \\ \left\|P_w u - \tilde{P}_w u\right\|_{L^2} &\leq C_{w,N} h^{N+2} \|w\|_{W^{N+1,\infty}} \|u\|_{W^{N+1,2}}.\end{aligned}$$

- WADG retains high order accuracy for moments: if $v \in P^M$

$$\left|\boldsymbol{v}^T\boldsymbol{M}_w\boldsymbol{u} - \boldsymbol{v}^T\boldsymbol{M}^{-1}\boldsymbol{M}_{1/w}\boldsymbol{M}^{-1}\boldsymbol{u}\right| \leq$$
$$C_w \|w\|_{W^{N+1,\infty}} h^{2N+2-M} \|u\|_{W^{N+1,2}} \|v\|_{L^2}.$$

# Acoustic wave equation: variable coefficients

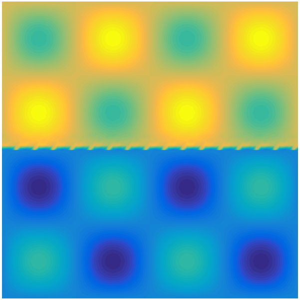

(a) Weight $w = c^2(x, y)$

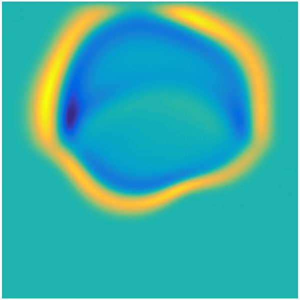

(b) Standard DG

Figure: Standard vs. weight-adjusted DG with spatially varying $c^2$ containing both smooth variations and a discontinuity.

# Acoustic wave equation: variable coefficients

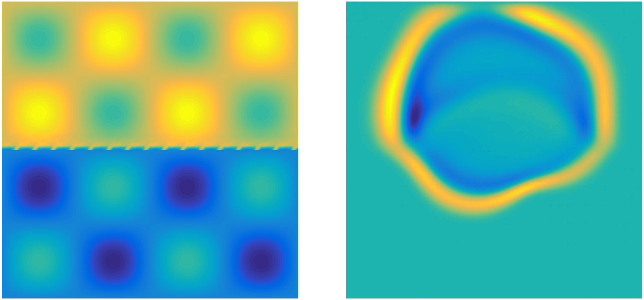

(a) Weight $w = c^2(x, y)$ (b) Weighted-adjusted DG

Figure: Standard vs. weight-adjusted DG with spatially varying $c^2$ containing both smooth variations and a discontinuity.

# Low storage WADG: efficiency on GPUs

| | $N = 1$ | $N = 2$ | $N = 3$ | $N = 4$ | $N = 5$ | $N = 6$ | $N = 7$ |
|---|---|---|---|---|---|---|---|
| $\boldsymbol{M}_w^{-1}$ | .66 | 2.79 | 9.90 | 29.4 | 73.9 | 170.5 | 329.4 |
| WADG | 0.59 | 1.44 | 4.30 | 13.9 | 43.0 | 107.8 | 227.7 |
| Speedup | 1.11 | 1.94 | 2.30 | 2.16 | 1.72 | 1.58 | 1.45 |

Time (ns) per element: storing/applying $\boldsymbol{M}_{1/w}^{-1}$ vs WADG (deg. $2N$ quadrature).

- Efficiency on GPUs: reduce memory accesses and data movement.
- (Tuned) low storage WADG faster than storing and applying $\boldsymbol{M}_{1/w}^{-1}$!

# Outline

# Matrix-valued weights and elastic wave propagation

- Symmetric hyperbolic system: velocity $\boldsymbol{v}$, stress $\boldsymbol{\sigma} = \mathrm{vec}(\boldsymbol{S})$ with $\boldsymbol{\sigma} = (\sigma_{xx}, \sigma_{yy}, \sigma_{zz}, \sigma_{yz}, \sigma_{xz}, \sigma_{xy})^T$.

$$\rho \frac{\partial \boldsymbol{v}}{\partial t} = \sum_{i=1}^{d} \boldsymbol{A}_i^T \frac{\partial \boldsymbol{\sigma}}{\partial \boldsymbol{x}_i}, \qquad \boldsymbol{C}^{-1} \frac{\partial \boldsymbol{\sigma}}{\partial t} = \sum_{i=1}^{d} \boldsymbol{A}_i \frac{\partial \boldsymbol{v}}{\partial \boldsymbol{x}_i}.$$

- Factoring out the constitutive stiffness tensor $\boldsymbol{C}$ results in simple and spatially constant matrices $\boldsymbol{A}_i$.

$$\boldsymbol{C} = \underbrace{\begin{pmatrix} 2\mu+\lambda & \lambda & \lambda & \\ \lambda & 2\mu+\lambda & \lambda & \\ \lambda & \lambda & 2\mu+\lambda & \\ & & & \mu \boldsymbol{I}_{3\times 3} \end{pmatrix}}_{\text{for isotropic media}}, \quad \boldsymbol{A}_1 = \begin{pmatrix} 1 & 0 & 0 \\ 0 & 0 & 0 \\ 0 & 0 & 0 \\ 0 & 0 & 0 \\ 0 & 0 & 1 \\ 0 & 1 & 0 \end{pmatrix}.$$

Hughes and Marsden 1978. Classical elastodynamics as a linear symmetric hyperbolic system.

# DG formulation for elasticity: energy stability

- Analogous to acoustics: numerical fluxes independent of media!

$$\int_{D^k}\left(\boldsymbol{C}^{-1}\frac{\partial\boldsymbol{\sigma}}{\partial t}\right)^T\boldsymbol{q} = \int_{D^k}\sum_{i=1}^{d}\boldsymbol{A}_i\frac{\partial\boldsymbol{v}}{\partial\boldsymbol{x}_i}\boldsymbol{q} + \frac{1}{2}\int_{\partial D^k}\left(\boldsymbol{A}_n\left[\!\left[\boldsymbol{v}\right]\!\right] + \tau_\sigma\boldsymbol{A}_n\boldsymbol{A}_n^T\left[\!\left[\boldsymbol{\sigma}\right]\!\right]\right)\boldsymbol{q},$$

$$\int_{D^k}\left(\rho\frac{\partial\boldsymbol{v}}{\partial t}\right)^T\boldsymbol{w} = \int_{D^k}\sum_{i=1}^{d}\boldsymbol{A}_i^T\frac{\partial\boldsymbol{\sigma}}{\partial\boldsymbol{x}_i}\boldsymbol{w} + \frac{1}{2}\int_{\partial D^k}\left(\boldsymbol{A}_n^T\left[\!\left[\boldsymbol{\sigma}\right]\!\right] + \tau_v\boldsymbol{A}_n^T\boldsymbol{A}_n\left[\!\left[\boldsymbol{v}\right]\!\right]\right)\boldsymbol{w}.$$

- Energy method: take $\boldsymbol{q} = \boldsymbol{\sigma}$, $\boldsymbol{w} = \boldsymbol{v}$

$$\int_{D^k}\left(\boldsymbol{C}^{-1}\frac{\partial\boldsymbol{\sigma}}{\partial t}\right)^T\boldsymbol{\sigma} = \frac{\partial}{\partial t}\int_{D^k}\left(\boldsymbol{\sigma}(\boldsymbol{x})^T\boldsymbol{C}^{-1}(\boldsymbol{x})\boldsymbol{\sigma}(\boldsymbol{x})\right)$$
$$\int_{D^k}\left(\boldsymbol{\rho}\frac{\partial\boldsymbol{v}}{\partial t}\right)^T\boldsymbol{v} = \frac{\partial}{\partial t}\int_{D^k}\rho(\boldsymbol{x})\left|\boldsymbol{v}\right|^2.$$

# DG formulation for elasticity: energy stability, cont.

- $\boldsymbol{A}_i$ constant, integration by parts if quadrature exact for degree $(2N-1)$

$$\int_{D^k} \sum_{i=1}^{d} \boldsymbol{A}_i \frac{\partial \boldsymbol{v}}{\partial \boldsymbol{x}_i} \cdot \boldsymbol{q} + \frac{1}{2} \int_{\partial D^k} \left( \boldsymbol{A}_n [\![ \boldsymbol{v} ]\!] + \tau_\sigma \boldsymbol{A}_n \boldsymbol{A}_n^T [\![ \boldsymbol{\sigma} ]\!] \right) \cdot \boldsymbol{q},$$

$$\int_{D^k} \sum_{i=1}^{d} \boldsymbol{A}_i^T \frac{\partial \boldsymbol{\sigma}}{\partial \boldsymbol{x}_i} \cdot \boldsymbol{w} + \frac{1}{2} \int_{\partial D^k} \left( \boldsymbol{A}_n^T [\![ \boldsymbol{\sigma} ]\!] + \tau_v \boldsymbol{A}_n^T \boldsymbol{A}_n [\![ \boldsymbol{v} ]\!] \right) \cdot \boldsymbol{w}$$

- Energy stability (penalty weakly enforces continuity conditions):

$$\sum_{D^k} \frac{1}{2} \frac{\partial}{\partial t} \int_{D^k} \rho \left| \boldsymbol{v} \right|^2 + \boldsymbol{\sigma}^T \boldsymbol{C}^{-1} \boldsymbol{\sigma} = - \sum_{\text{faces}} \int_f \frac{\tau_{\boldsymbol{v}}}{2} \left| \boldsymbol{A}_n [\![ \boldsymbol{v} ]\!] \right|^2 + \frac{\tau_{\boldsymbol{\sigma}}}{2} \left| \boldsymbol{A}_n^T [\![ \boldsymbol{\sigma} ]\!] \right|^2 \leq 0.$$

- $\tau_v, \tau_\sigma > 0$ penalizes normal jumps $[\![ \boldsymbol{v} ]\!] \cdot \boldsymbol{n} \approx 0$, $[\![ \boldsymbol{S} ]\!] \cdot \boldsymbol{n} \approx 0$.

# DG formulation for elasticity: energy stability, cont.

- $\boldsymbol{A}_i$ constant, integration by parts if quadrature exact for degree $(2N-1)$

$$\int_{D^k} \sum_{i=1}^{d} -\boldsymbol{v} \cdot \boldsymbol{A}_i^T \frac{\partial \boldsymbol{q}}{\partial \boldsymbol{x}_i} + \int_{\partial D^k} \left( \boldsymbol{A}_n \{\{\boldsymbol{v}\}\} + \frac{\tau_\sigma}{2} \boldsymbol{A}_n \boldsymbol{A}_n^T [\![\boldsymbol{\sigma}]\!] \right) \cdot \boldsymbol{q},$$

$$\int_{D^k} \sum_{i=1}^{d} \boldsymbol{A}_i^T \frac{\partial \boldsymbol{\sigma}}{\partial \boldsymbol{x}_i} \cdot \boldsymbol{w} + \frac{1}{2} \int_{\partial D^k} \left( \boldsymbol{A}_n^T [\![\boldsymbol{\sigma}]\!] + \tau_v \boldsymbol{A}_n^T \boldsymbol{A}_n [\![\boldsymbol{v}]\!] \right) \cdot \boldsymbol{w}$$

- Energy stability (penalty weakly enforces continuity conditions):

$$\sum_{D^k} \frac{1}{2} \frac{\partial}{\partial t} \int_{D^k} \rho \left|\boldsymbol{v}\right|^2 + \boldsymbol{\sigma}^T \boldsymbol{C}^{-1} \boldsymbol{\sigma} =$$

$$- \sum_{\text{faces}} \int_f \frac{\tau_{\boldsymbol{v}}}{2} \left|\boldsymbol{A}_n [\![\boldsymbol{v}]\!]\right|^2 + \frac{\tau_{\boldsymbol{\sigma}}}{2} \left|\boldsymbol{A}_n^T [\![\boldsymbol{\sigma}]\!]\right|^2 \leq 0.$$

- $\tau_v, \tau_\sigma > 0$ penalizes normal jumps $[\![\boldsymbol{v}]\!] \cdot \boldsymbol{n} \approx 0$, $[\![\boldsymbol{S}]\!] \cdot \boldsymbol{n} \approx 0$.

# DG formulation for elasticity: energy stability, cont.

- $\boldsymbol{A}_i$ constant, integration by parts if quadrature exact for degree $(2N-1)$

$$\int_{D^k} \sum_{i=1}^{d} -\boldsymbol{v} \cdot \boldsymbol{A}_i^T \frac{\partial \boldsymbol{\sigma}}{\partial \boldsymbol{x}_i} + \int_{\partial D^k} \left( \boldsymbol{A}_n \{\{\boldsymbol{v}\}\} + \frac{\tau_\sigma}{2} \boldsymbol{A}_n \boldsymbol{A}_n^T [\![\boldsymbol{\sigma}]\!] \right) \cdot \boldsymbol{\sigma},$$

$$\int_{D^k} \sum_{i=1}^{d} \boldsymbol{A}_i^T \frac{\partial \boldsymbol{\sigma}}{\partial \boldsymbol{x}_i} \cdot \boldsymbol{v} + \frac{1}{2} \int_{\partial D^k} \left( \boldsymbol{A}_n^T [\![\boldsymbol{\sigma}]\!] + \tau_v \boldsymbol{A}_n^T \boldsymbol{A}_n [\![\boldsymbol{v}]\!] \right) \cdot \boldsymbol{v}$$

- Energy stability (penalty weakly enforces continuity conditions):

$$\sum_{D^k} \frac{1}{2} \frac{\partial}{\partial t} \int_{D^k} \rho \left|\boldsymbol{v}\right|^2 + \boldsymbol{\sigma}^T \boldsymbol{C}^{-1} \boldsymbol{\sigma} =$$

$$- \sum_{\text{faces}} \int_f \frac{\tau_{\boldsymbol{v}}}{2} \left|\boldsymbol{A}_n [\![\boldsymbol{v}]\!]\right|^2 + \frac{\tau_{\boldsymbol{\sigma}}}{2} \left|\boldsymbol{A}_n^T [\![\boldsymbol{\sigma}]\!]\right|^2 \leq 0.$$

- $\tau_v, \tau_\sigma > 0$ penalizes normal jumps $[\![\boldsymbol{v}]\!] \cdot \boldsymbol{n} \approx 0$, $[\![\boldsymbol{S}]\!] \cdot \boldsymbol{n} \approx 0$.

# DG formulation for elasticity: energy stability, cont.

- $\boldsymbol{A}_i$ constant, integration by parts if quadrature exact for degree $(2N-1)$

$$\text{Sum volume terms, which cancel to zero} +$$

$$\int_{\partial D^k} \left(\boldsymbol{A}_n \{\{\boldsymbol{v}\}\} + \frac{\tau_\sigma}{2}\boldsymbol{A}_n\boldsymbol{A}_n^T [\![\boldsymbol{\sigma}]\!]\right)\cdot\boldsymbol{\sigma} + \frac{1}{2}\left(\boldsymbol{A}_n^T [\![\boldsymbol{\sigma}]\!] + \tau_v\boldsymbol{A}_n^T\boldsymbol{A}_n [\![\boldsymbol{v}]\!]\right)\cdot\boldsymbol{v}$$

- Energy stability (penalty weakly enforces continuity conditions):

$$\sum_{D^k}\frac{1}{2}\frac{\partial}{\partial t}\int_{D^k}\rho\left|\boldsymbol{v}\right|^2 + \boldsymbol{\sigma}^T\boldsymbol{C}^{-1}\boldsymbol{\sigma} =$$

$$-\sum_{\text{faces}}\int_f \frac{\tau_{\boldsymbol{v}}}{2}\left|\boldsymbol{A}_n [\![\boldsymbol{v}]\!]\right|^2 + \frac{\tau_{\boldsymbol{\sigma}}}{2}\left|\boldsymbol{A}_n^T [\![\boldsymbol{\sigma}]\!]\right|^2 \leq 0.$$

- $\tau_v, \tau_\sigma > 0$ penalizes normal jumps $[\![\boldsymbol{v}]\!]\cdot\boldsymbol{n}\approx 0$, $[\![\boldsymbol{S}]\!]\cdot\boldsymbol{n}\approx 0$.

# DG formulation for elasticity: energy stability, cont.

- $\boldsymbol{A}_i$ constant, integration by parts if quadrature exact for degree $(2N-1)$

Sum volume terms, which cancel to zero +

$$\int_{\partial D^k} \left( \boldsymbol{A}_n \{\{\boldsymbol{v}\}\} + \frac{\tau_\sigma}{2} \boldsymbol{A}_n \boldsymbol{A}_n^T [\![\boldsymbol{\sigma}]\!] \right) \cdot \boldsymbol{\sigma} + \frac{1}{2} \left( \boldsymbol{A}_n^T [\![\boldsymbol{\sigma}]\!] + \tau_v \boldsymbol{A}_n^T \boldsymbol{A}_n [\![\boldsymbol{v}]\!] \right) \cdot \boldsymbol{v}$$

- Energy stability (penalty weakly enforces continuity conditions):

$$\sum_{D^k} \frac{1}{2} \frac{\partial}{\partial t} \int_{D^k} \rho \left|\boldsymbol{v}\right|^2 + \boldsymbol{\sigma}^T \boldsymbol{C}^{-1} \boldsymbol{\sigma} =$$

$$- \sum_{\text{faces}} \int_f \frac{\tau_{\boldsymbol{v}}}{2} \left|\boldsymbol{A}_n [\![\boldsymbol{v}]\!]\right|^2 + \frac{\tau_{\boldsymbol{\sigma}}}{2} \left|\boldsymbol{A}_n^T [\![\boldsymbol{\sigma}]\!]\right|^2 \leq 0.$$

- $\tau_v, \tau_\sigma > 0$ penalizes normal jumps $[\![\boldsymbol{v}]\!] \cdot \boldsymbol{n} \approx 0$, $[\![\boldsymbol{S}]\!] \cdot \boldsymbol{n} \approx 0$.

# DG formulation for elasticity: energy stability, cont.

- $\boldsymbol{A}_i$ constant, integration by parts if quadrature exact for degree $(2N-1)$

Sum over all elements: central flux terms cancel +

$$\sum_k \int_{\partial D^k} \frac{\tau_\sigma}{2} \boldsymbol{A}_n \boldsymbol{A}_n^T [\![\boldsymbol{\sigma}]\!] \cdot \boldsymbol{\sigma} + \frac{\tau_v}{2} \boldsymbol{A}_n^T \boldsymbol{A}_n [\![\boldsymbol{v}]\!] \cdot \boldsymbol{v}$$

- Energy stability (penalty weakly enforces continuity conditions):

$$\sum_{D^k} \frac{1}{2} \frac{\partial}{\partial t} \int_{D^k} \rho |\boldsymbol{v}|^2 + \boldsymbol{\sigma}^T \boldsymbol{C}^{-1} \boldsymbol{\sigma} =$$
$$- \sum_{\text{faces}} \int_f \frac{\tau_{\boldsymbol{v}}}{2} |\boldsymbol{A}_n [\![\boldsymbol{v}]\!]|^2 + \frac{\tau_{\boldsymbol{\sigma}}}{2} \left| \boldsymbol{A}_n^T [\![\boldsymbol{\sigma}]\!] \right|^2 \leq 0.$$

- $\tau_v, \tau_\sigma > 0$ penalizes normal jumps $[\![\boldsymbol{v}]\!] \cdot \boldsymbol{n} \approx 0$, $[\![\boldsymbol{S}]\!] \cdot \boldsymbol{n} \approx 0$.

# DG formulation for elasticity: energy stability, cont.

- $\boldsymbol{A}_i$ constant, integration by parts if quadrature exact for degree $(2N-1)$

Sum over all elements: combine penalty flux terms+

$$\sum_k \int_{\partial D^k} \frac{\tau_\sigma}{2} \boldsymbol{A}_n^T [\![\boldsymbol{\sigma}]\!] \cdot \boldsymbol{A}_n^T \boldsymbol{\sigma} + \frac{\tau_v}{2} \boldsymbol{A}_n [\![\boldsymbol{v}]\!] \cdot \boldsymbol{A}_n \boldsymbol{v}$$

- Energy stability (penalty weakly enforces continuity conditions):

$$\sum_{D^k} \frac{1}{2} \frac{\partial}{\partial t} \int_{D^k} \rho \left|\boldsymbol{v}\right|^2 + \boldsymbol{\sigma}^T \boldsymbol{C}^{-1} \boldsymbol{\sigma} =$$

$$- \sum_{\text{faces}} \int_f \frac{\tau_{\boldsymbol{v}}}{2} \left|\boldsymbol{A}_n [\![\boldsymbol{v}]\!]\right|^2 + \frac{\tau_{\boldsymbol{\sigma}}}{2} \left|\boldsymbol{A}_n^T [\![\boldsymbol{\sigma}]\!]\right|^2 \leq 0.$$

- $\tau_v, \tau_\sigma > 0$ penalizes normal jumps $[\![\boldsymbol{v}]\!] \cdot \boldsymbol{n} \approx 0$, $[\![\boldsymbol{S}]\!] \cdot \boldsymbol{n} \approx 0$.

# DG formulation for elasticity: energy stability, cont.

- $\boldsymbol{A}_i$ constant, integration by parts if quadrature exact for degree $(2N-1)$

Sum over all elements: combine penalty flux terms+

$$\sum_k \int_{\partial D^k} \frac{\tau_\sigma}{2} \boldsymbol{A}_n^T [\![\boldsymbol{\sigma}]\!] \cdot \boldsymbol{A}_n^T [\![\boldsymbol{\sigma}]\!] + \frac{\tau_v}{2} \boldsymbol{A}_n [\![\boldsymbol{v}]\!] \cdot \boldsymbol{A}_n [\![\boldsymbol{v}]\!]$$

- Energy stability (penalty weakly enforces continuity conditions):

$$\sum_{D^k} \frac{1}{2} \frac{\partial}{\partial t} \int_{D^k} \rho |\boldsymbol{v}|^2 + \boldsymbol{\sigma}^T \boldsymbol{C}^{-1} \boldsymbol{\sigma} =$$

$$- \sum_{\text{faces}} \int_f \frac{\tau_{\boldsymbol{v}}}{2} |\boldsymbol{A}_n [\![\boldsymbol{v}]\!]|^2 + \frac{\tau_{\boldsymbol{\sigma}}}{2} \left| \boldsymbol{A}_n^T [\![\boldsymbol{\sigma}]\!] \right|^2 \leq 0.$$

- $\tau_v, \tau_\sigma > 0$ penalizes normal jumps $[\![\boldsymbol{v}]\!] \cdot \boldsymbol{n} \approx 0$, $[\![\boldsymbol{S}]\!] \cdot \boldsymbol{n} \approx 0$.

# DG formulation for elasticity: energy stability, cont.

- $\boldsymbol{A}_i$ constant, integration by parts if quadrature exact for degree $(2N-1)$

Sum over all elements: combine penalty flux terms+

$$\sum_k \int_{\partial D^k} \frac{\tau_\sigma}{2} \boldsymbol{A}_n^T [\![\boldsymbol{\sigma}]\!] \cdot \boldsymbol{A}_n^T [\![\boldsymbol{\sigma}]\!] + \frac{\tau_v}{2} \boldsymbol{A}_n [\![\boldsymbol{v}]\!] \cdot \boldsymbol{A}_n [\![\boldsymbol{v}]\!]$$

…and done!

- Energy stability (penalty weakly enforces continuity conditions):

$$\sum_{D^k} \frac{1}{2} \frac{\partial}{\partial t} \int_{D^k} \rho \left|\boldsymbol{v}\right|^2 + \boldsymbol{\sigma}^T \boldsymbol{C}^{-1} \boldsymbol{\sigma} = - \sum_{\text{faces}} \int_f \frac{\tau_{\boldsymbol{v}}}{2} \left|\boldsymbol{A}_n [\![\boldsymbol{v}]\!]\right|^2 + \frac{\tau_{\boldsymbol{\sigma}}}{2} \left|\boldsymbol{A}_n^T [\![\boldsymbol{\sigma}]\!]\right|^2 \leq 0.$$

- $\tau_v, \tau_\sigma > 0$ penalizes normal jumps $[\![\boldsymbol{v}]\!] \cdot \boldsymbol{n} \approx 0$, $[\![\boldsymbol{S}]\!] \cdot \boldsymbol{n} \approx 0$.

# Semi-discrete system: matrix-valued weighted

- Matrix-weighted mass matrix: let $\boldsymbol{W} \in \mathbb{R}^{d \times d}$ be SPD with entries $w_{ij}$

$$\boldsymbol{M}_{\boldsymbol{W}} = \begin{pmatrix} \boldsymbol{M}_{w_{11}} & \dots & \boldsymbol{M}_{w_{1d}} \\ \vdots & \ddots & \vdots \\ \boldsymbol{M}_{w_{d1}} & \dots & \boldsymbol{M}_{w_{dd}} \end{pmatrix}$$

- Semi-discrete DG formulation involves $\boldsymbol{C}^{-1}$-weighted mass matrix

$$\boldsymbol{M}_{\boldsymbol{C}^{-1}} \frac{\partial \boldsymbol{\Sigma}}{\partial t} = \sum_{i=1}^{d} (\boldsymbol{A}_i \otimes \boldsymbol{S}_i) \boldsymbol{V} + \sum_{\text{faces}} \left( \boldsymbol{I} \otimes \boldsymbol{M}^f \right) \boldsymbol{F}_\sigma,$$

$$\boldsymbol{M}_{\rho \boldsymbol{I}} \frac{\partial \boldsymbol{V}}{\partial t} = \sum_{i=1}^{d} \left( \boldsymbol{A}_i^T \otimes \boldsymbol{S}_i \right) \boldsymbol{\Sigma} + \sum_{\text{faces}} \left( \boldsymbol{I} \otimes \boldsymbol{M}^f \right) \boldsymbol{F}_v.$$

# Weight-adjusted DG: matrix-valued weights

- Matrix-weighted mass matrix large, hard to invert

$$\boldsymbol{M}_{\boldsymbol{C}^{-1}} = \begin{pmatrix} \boldsymbol{M}_{\boldsymbol{C}_{11}^{-1}} & \cdots & \boldsymbol{M}_{\boldsymbol{C}_{1d}^{-1}} \\ \vdots & \ddots & \vdots \\ \boldsymbol{M}_{\boldsymbol{C}_{d1}^{-1}} & \cdots & \boldsymbol{M}_{\boldsymbol{C}_{dd}^{-1}} \end{pmatrix}$$

- Weight-adjusted approximation for $\boldsymbol{C}^{-1}$ decouples each component

$$\boldsymbol{M}_{\boldsymbol{C}^{-1}}^{-1} \approx \left(\boldsymbol{I} \otimes \boldsymbol{M}^{-1}\right) \boldsymbol{M}_{\boldsymbol{C}} \left(\boldsymbol{I} \otimes \boldsymbol{M}^{-1}\right).$$

- Evaluate RHS components at quadrature points, apply $\boldsymbol{C}(\boldsymbol{x}_i)$ to component vectors at quadrature points, project back to polynomials.

- Recovers Kronecker product $\boldsymbol{M}_{\boldsymbol{C}^{-1}}^{-1} = \boldsymbol{C} \otimes \boldsymbol{M}^{-1}$ for constant $\boldsymbol{C}^{-1}$.

# Energy stability and DG spectra

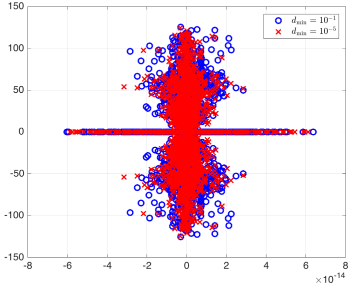


(a) Central flux ($\tau_v, \tau_\sigma = 0$)

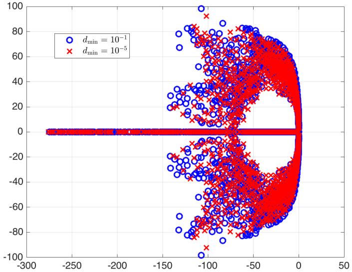


(b) Penalty flux ($\tau_v, \tau_\sigma = 1$)

Figure: DG spectra with random heterogeneities at each quadrature point.

- Guaranteed energy stability for both energy conservative and energy dissipative numerical interface fluxes.
- CFL can be improved by setting $\tau_\sigma \approx 1/\left\|\boldsymbol{C}\right\|$, $\tau_v \approx \left\|\rho\right\|$

# Elastic wave propagation: convergence

- Convergence for harmonic oscillation, Rayleigh, Lamb, and Stoneley waves: between $O(h^{N+1})$ and $O(h^{N+1/2})$.

- $\boldsymbol{\sigma}$ error grows as $\left\|\boldsymbol{C}^{-1}\right\| \to \infty$ (e.g. incompressible limit $\lambda/\mu \to \infty$).

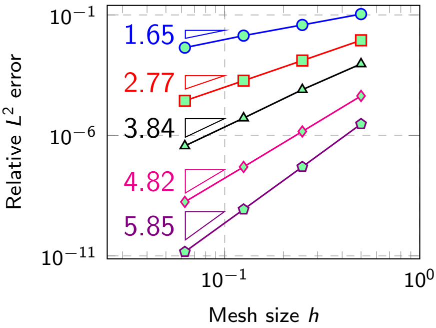


(a) $L^2$ errors (Stoneley wave)

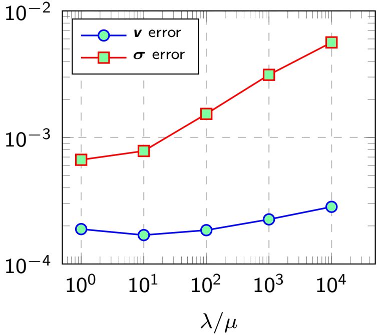


(b) $\left\|\boldsymbol{C}^{-1}\right\| \to \infty$, $N = 3, h = 1/8$.

# Elastic wave propagation: stiff inclusion

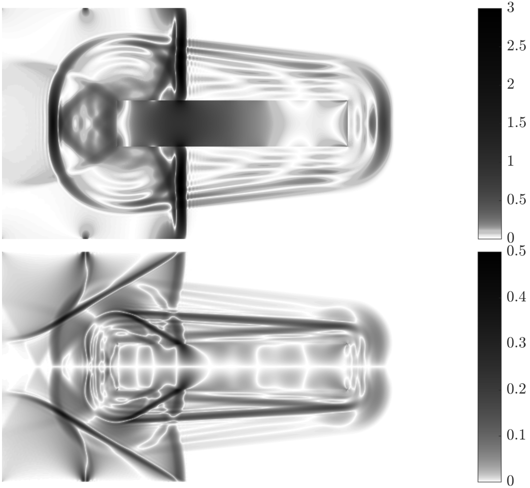


Figure: $\mathrm{tr}(\boldsymbol{\sigma})$ and $\boldsymbol{\sigma}_{xy}$ for stiff inclusion with $N = 5$, $h \approx 1/50$.

# Elastic wave propagation: anisotropy

Simple implementation for anisotropy - fluxes independent of $\boldsymbol{C}$.

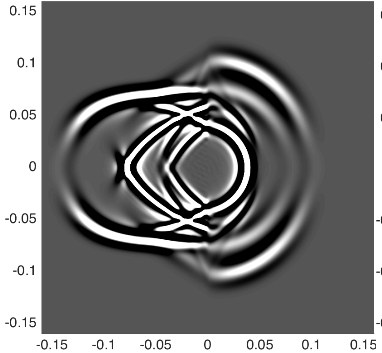


(a) Vertical velocity, $t = 30\mu s$

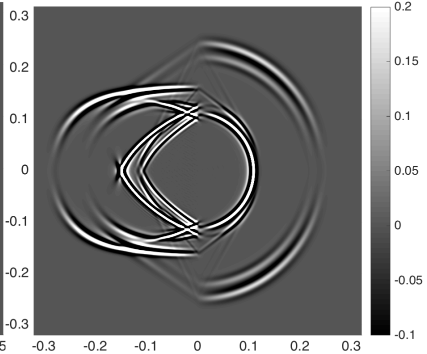


(b) Vertical velocity, $t = 60\mu s$

Anisotropic heterogeneous media: transverse isotropy ($x < 0$), isotropy ($x > 0$).

Komatitsch, Barnes, Tromp 2000. Simulation of anisotropic wave propagation based upon a spectral element method.

# Curved meshes and heterogeneous media

- Map curved elements $D^k$ to reference element $\hat{D}$, introduce determinant of Jacobian of mapping $J$ (varies of $\hat{D}$).
- RHS terms: discretize skew-symmetric form

$$\int_{\hat{D}} \sum_{i=1}^{d} -\boldsymbol{v} \cdot \boldsymbol{A}_i^T \frac{\partial \boldsymbol{q}}{\partial \boldsymbol{x}_i} J + \int_{\partial D^k} \left( \boldsymbol{A}_n \{\{\boldsymbol{v}\}\} + \frac{\tau_\sigma}{2} \boldsymbol{A}_n \boldsymbol{A}_n^T [\![\boldsymbol{\sigma}]\!] \right) \boldsymbol{q},$$

$$\int_{\hat{D}} \sum_{i=1}^{d} \boldsymbol{A}_i^T \frac{\partial \boldsymbol{\sigma}}{\partial \boldsymbol{x}_i} \cdot \boldsymbol{w} J + \frac{1}{2} \int_{\partial D^k} \left( \boldsymbol{A}_n^T [\![\boldsymbol{\sigma}]\!] + \tau_v \boldsymbol{A}_n^T \boldsymbol{A}_n [\![\boldsymbol{v}]\!] \right) \boldsymbol{w}.$$

- Time-derivative terms: $J$ incorporated into matrix weighting.

$$\int_{D^k} \left( \boldsymbol{C}^{-1} \frac{\partial \boldsymbol{\sigma}}{\partial t} \right)^T \boldsymbol{q} = \int_{\hat{D}} \left( J \boldsymbol{C}^{-1} \frac{\partial \boldsymbol{\sigma}}{\partial t} \right)^T \boldsymbol{q}.$$

# Curved meshes and random heterogeneous media

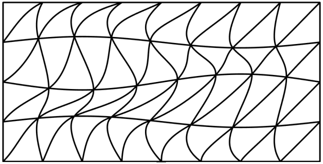

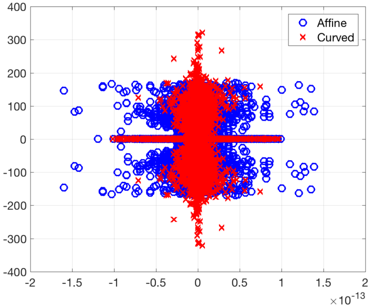


(b) Central flux ($\tau_v, \tau_\sigma = 0$)

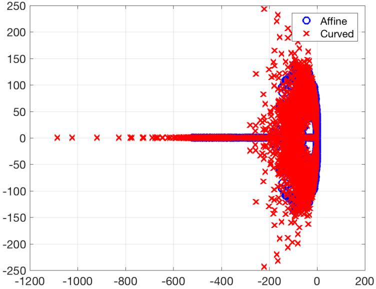


(c) Central flux ($\tau_v, \tau_\sigma = 1$)

A skew-symmetric discretization guarantees discrete energy stability.

# Elastic wave propagation: 3D isotropic media

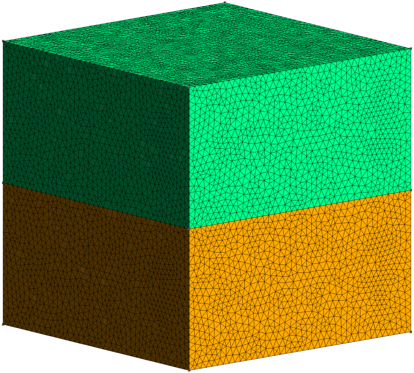

(a) Computational mesh

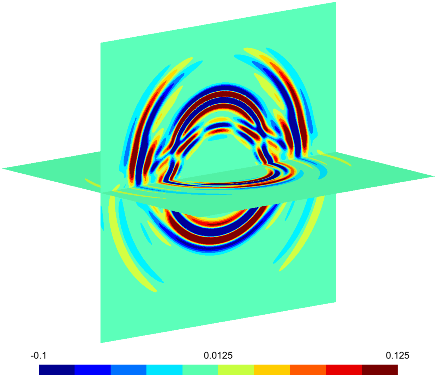


(b) Homogeneous isotropic media

Figure: $\mathrm{tr}(\boldsymbol{\sigma})$ with $\mu(\boldsymbol{x}) = 1 + H(y) + \frac{1}{2}\cos(3\pi x)\cos(3\pi y)\cos(3\pi z)$, $N = 5$.

# Elastic wave propagation: 3D isotropic media

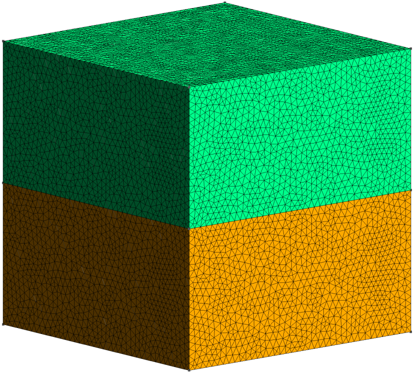

(a) Computational mesh

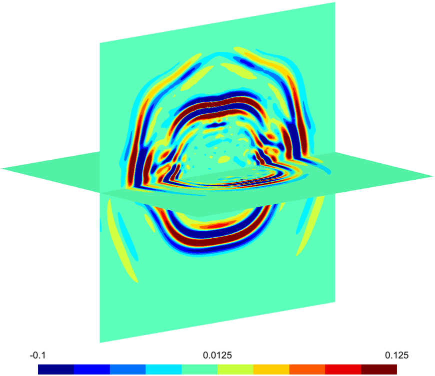


(b) Piecewise constant $\boldsymbol{C}(\boldsymbol{x})$

Figure: $\mathrm{tr}(\boldsymbol{\sigma})$ with $\mu(\boldsymbol{x}) = 1 + H(y) + \frac{1}{2}\cos(3\pi x)\cos(3\pi y)\cos(3\pi z)$, $N = 5$.

# Elastic wave propagation: 3D isotropic media

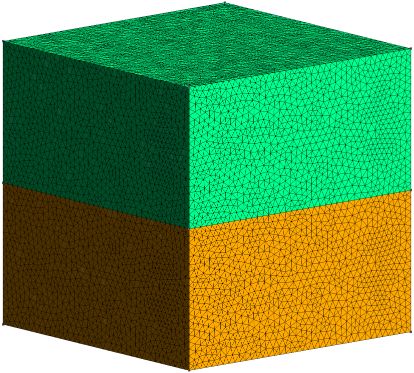

(a) Computational mesh

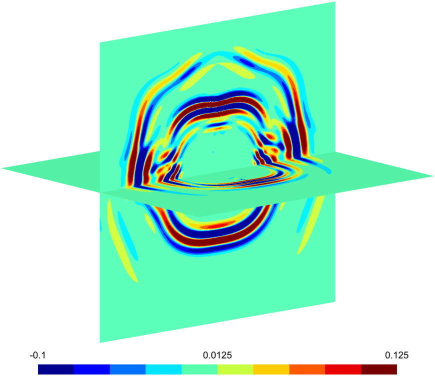


(b) High order $\boldsymbol{C}(\boldsymbol{x})$

Figure: $\mathrm{tr}(\boldsymbol{\sigma})$ with $\mu(\boldsymbol{x}) = 1 + H(y) + \frac{1}{2}\cos(3\pi x)\cos(3\pi y)\cos(3\pi z)$, $N = 5$.

# Outline

# Acoustic-elastic coupling

- Coupling conditions for fluid (acoustic) and solid (elastic) media:

$$\boldsymbol{S} \cdot \boldsymbol{n} = p\boldsymbol{n}, \qquad \boldsymbol{v} \cdot \boldsymbol{n} = \boldsymbol{u} \cdot \boldsymbol{n}.$$

- Replace $[\![p]\!]$ and $[\![\boldsymbol{\sigma}]\!]$ with residuals of coupling conditions

$$\begin{aligned} [\![p]\!] &= \boldsymbol{n} \cdot \left(\boldsymbol{S}^{+} \cdot \boldsymbol{n}\right) - p, && \text{(acoustic side)} \\ \boldsymbol{A}_n^T [\![\boldsymbol{\sigma}]\!] = [\![\boldsymbol{S}]\!] \cdot \boldsymbol{n} &= p^{+}\boldsymbol{n} - \boldsymbol{S} \cdot \boldsymbol{n}, && \text{(elastic side).} \end{aligned}$$

- Energy stable for arbitrary acoustic and elastic media.

# Acoustic-elastic coupling: arbitrary heterogeneous media

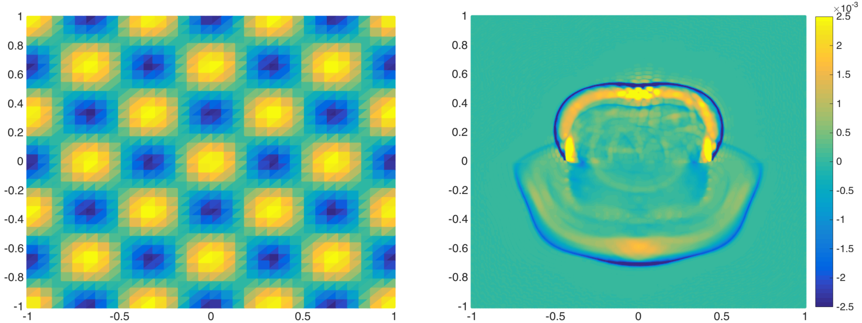


(a) Low order $c^2(\boldsymbol{x}), \mu(\boldsymbol{x})$ (b) $\mathrm{tr}(\boldsymbol{\sigma})$

Figure: Acoustic-elastic waves from a Ricker pulse ($N = 10$, $h = 1/16$).

# Acoustic-elastic coupling: arbitrary heterogeneous media

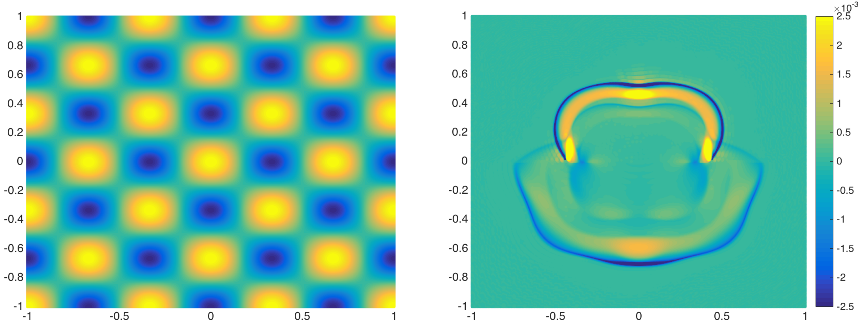


(a) High order $c^2(\boldsymbol{x}), \mu(\boldsymbol{x})$ (b) $\mathrm{tr}(\boldsymbol{\sigma})$

Figure: Acoustic-elastic waves from a Ricker pulse ($N = 10$, $h = 1/16$).

# Poroelasticity: low frequency Biot's system

- Biot's system adds pore pressure $p$ and relative fluid velocity $\boldsymbol{q}$.
- Symmetric first order system with augmented stress, velocity.

$$\tilde{\boldsymbol{\sigma}} = \left(\sigma_{xx}, \sigma_{yy}, \sigma_{zz}, \sigma_{yz}, \sigma_{xz}, \sigma_{xy}, p\right)^T, \quad \tilde{\boldsymbol{v}} = \left(v_x, v_y, v_z, q_x, q_y, q_z\right)^T$$

$$\boldsymbol{E}_v \frac{\partial \tilde{\boldsymbol{v}}}{\partial t} = \sum_{i=1}^{d} \boldsymbol{A}_i^T \frac{\partial \tilde{\boldsymbol{\sigma}}}{\partial \boldsymbol{x}_i} - \boldsymbol{D}\tilde{\boldsymbol{v}}, \qquad \boldsymbol{E}_\sigma \frac{\partial \tilde{\boldsymbol{\sigma}}}{\partial t} = \sum_{i=1}^{d} \boldsymbol{A}_i \frac{\partial \tilde{\boldsymbol{v}}}{\partial \boldsymbol{x}_i}.$$

- $\boldsymbol{E}_s, \boldsymbol{E}_v$ SPD, $\boldsymbol{A}_i$ spatially const. $+$ sparse (a single $\pm 1$ per row).

$$\boldsymbol{E}_v = \begin{pmatrix} \rho & & \rho_f & \\ & \ddots & & \ddots \\ \rho_f & & m_1 & \\ & \ddots & & \ddots \end{pmatrix}, \quad \boldsymbol{E}_s = \begin{pmatrix} \boldsymbol{C}^{-1} & \boldsymbol{C}^{-1}\boldsymbol{\alpha} \\ \boldsymbol{\alpha}^T \boldsymbol{C}^{-1} & \frac{1}{M} + \boldsymbol{\alpha}^T \boldsymbol{C}^{-1}\boldsymbol{\alpha} \end{pmatrix},$$

Lemoine, Ou, LeVeque 2013. High-resolution finite volume modeling of wave propagation in orthotropic poroelastic media.

# Numerical results for Biot (with de Hoop, Shukla)

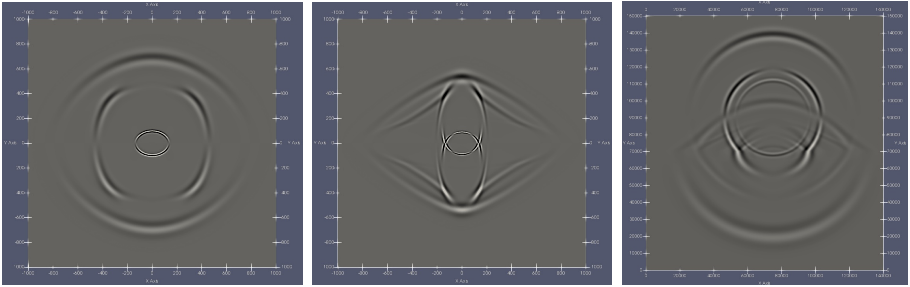

(a) Orthotropic media, 1.56 ms (b) Epoxy-glass, 1.8 ms (c) Isotropic interface, 230 ms

Inviscid Biot solution (mass particle velocity) showing fast P, slow S, and slow P waves. Simulation utilizes $N = 3$ and a uniform mesh of 128 elements per side.

Systematic derivation of WADG formulations: can symmetrize a system by defining an appropriate convex entropy (energy function).

Carcione 1996. Wave propagation in anisotropic, saturated porous media: plane wave theory and numerical simulation.
Lemoine, Ou, LeVeque 2013. High-resolution finite volume modeling of wave propagation in orthotropic poroelastic media.

# Summary and acknowledgements

- Weight-adjusted DG (WADG) for acoustic and elastic wave propagation in heterogeneous media and on curved meshes.
- Generalized mass lumping: energy stability and high order accuracy.
- Significantly simpler formulations using symmetric forms of PDEs.
- This work is supported by DMS-1719818 and DMS-1712639.

Thank you! Questions?

Chan, Hewett, Warburton. 2017. Weight-adjusted DG methods: wave propagation in heterogeneous media (SISC).

Chan 2018. Weight-adjusted DG methods: matrix-valued weights and elastic wave prop. in heterogeneous media (IJNME).

# Additional slides

# Computational costs at high orders of approximation

Note: WADG at high orders becomes **expensive**!

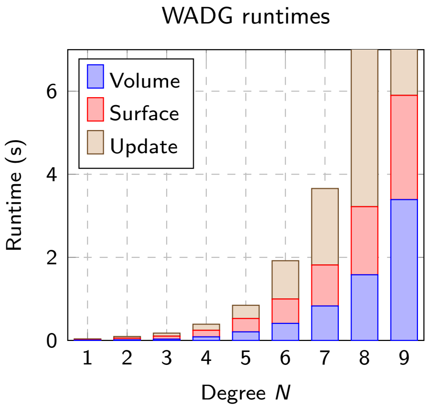


WADG runtimes for 50 timesteps, 98304 elements.

- Large **dense** matrices: $O(N^6)$ work per tet.
- High orders usually use tensor-product elements: $O(N^4)$ vs $O(N^6)$ cost, but less geometric flexibility.
- Idea: choose basis such that matrices are **sparse**.

# BBDG: efficient volume, surface kernels

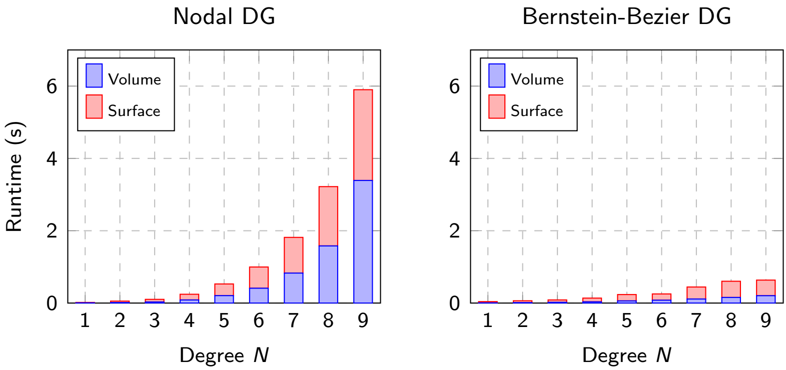


Bernstein-Bezier speedup requires constant coefficient RHS evaluation!

# BBDG: efficient volume, surface kernels

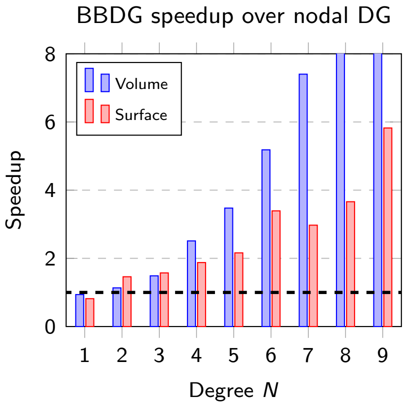


Bernstein-Bezier speedup requires constant coefficient RHS evaluation!

# BBWADG: polynomial multiplication and projection

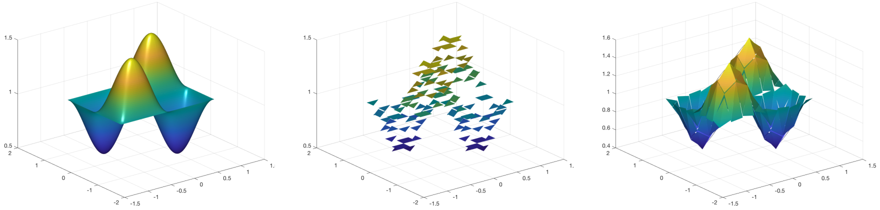

(a) Exact $c^2$ (b) $M = 0$ approximation (c) $M = 1$ approximation

- WADG reuses fast Bernstein volume and surface kernels.
- Fast $O(N^3)$ Bernstein algorithms for polynomial multiplication: represent $c^2 \in P^M$, $p(\boldsymbol{x}) \in P^N$, and construct $c^2(\boldsymbol{x})p(\boldsymbol{x}) \in P^{M+N}$.
- Fast $O(N^4)$ polynomial $L^2$ projection $\tilde{\boldsymbol{P}}_N : P^{M+N} \to P^N$.

# BBWADG: computational runtime for $M = 1$

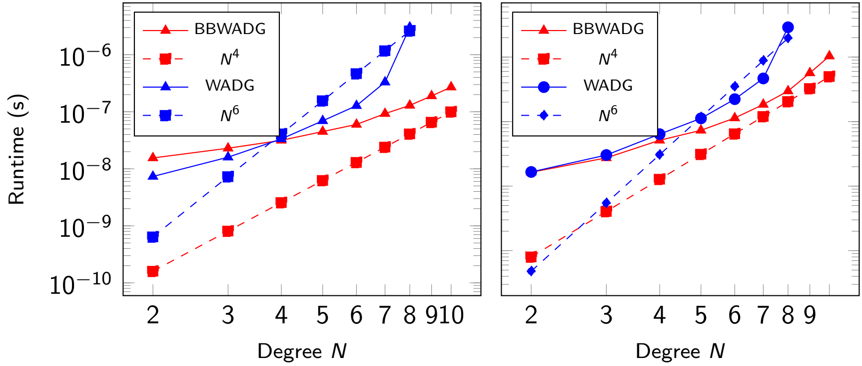


(a) (b)

# BBWADG: update kernel speedup over WADG (acoustics)

| | $N=3$ | $N=4$ | $N=5$ | $N=6$ | $N=7$ | $N=8$ |
|---|---|---|---|---|---|---|
| WADG | 1.60e-8 | 3.34e-8 | 6.94e-8 | 1.28e-7 | 3.31e-7 | 3.03e-6 |
| BBWADG | 2.20e-8 | 3.30e-8 | 4.42e-8 | 6.01e-8 | 9.46e-8 | 1.31e-7 |
| Speedup | 0.7260 | 1.0127 | 1.5706 | 2.1258 | 3.4938 | 23.1591 |

For $N \geq 8$, quadrature (and WADG) becomes much more expensive.

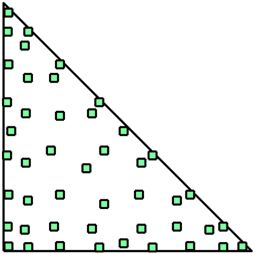

(a) $N = 7$ quadrature

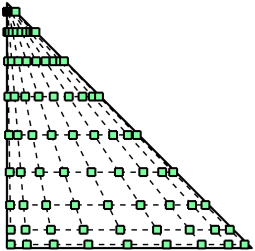

(b) $N = 8$ quadrature

# BBWADG: approximating $c^2$ and accuracy

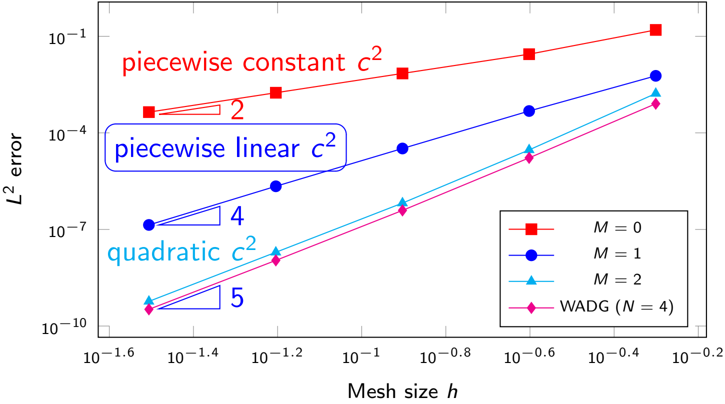


Approximating smooth $c^2(\boldsymbol{x})$ using $L^2$ projection:
$O(h^2)$ for $M = 0$, $O(h^4)$ for $M = 1$, $O(h^{M+3})$ for $0 < M \leq N - 2$.